*Biochimica et Biophysica Acta*, 597 (1980) 445—463


BBA 78699

# THE ORGANIZATION OF *n*-ALKANES IN LIPID BILAYERS

T.J. McINTOSH [a], S.A. SIMON [b] and R.C. MacDONALD [c]

[a] *Departments of Anatomy,* [b] *Physiology and Anesthesiology, Duke University Medical Center, Durham, NC 27710 and* [c] *Department of Biological Sciences, Northwestern University, Evanston, IL 60701 (U.S.A.)*

(Received July 23rd, 1979)

*Key words: n-Alkane; X-ray diffraction; Phase transition; Lipid organization; (Bilayer)*

## Summary

The interaction of *n*-alkanes (C6—C16) with phosphatidylcholine has been studied by the combined use of differential scanning calorimetry, X-ray diffraction and monolayer techniques. It has been found that the thermal properties and ultrastructure of lipid-alkane vesicles are strongly dependent on the length of the *n*-alkanes. Long alkanes, such as tetradecane and hexadecane, increase the transition temperature of dimyristoyl phosphatidylcholine and dipalmitoyl phosphatidylcholine, while the X-ray data indicate that these long alkanes align parallel to the lipid acyl chains. In contrast, shorter alkanes, such as hexane and octane, decrease and broaden the thermal transition and electron density profiles show that these alkanes increase bilayer width by partitioning between the apposing monolayers of the bilayer. For lipids in the gel and liquid crystalline states, the short alkanes form an alkane region in the geometric center of the bilayer.

## Introduction

The interaction of *n*-alkanes with lipid bilayers is of general interest for a variety of reasons. First of all, a knowledge of the manner in which alkanes are arranged in bilayers will further the understanding of how to treat the bilayer as a solvent for other molecules. The *n*-alkanes, especially the shorter ones, are anesthetics and have other pharmacological effects [1]. It has been postulated that this is due to an interaction with the bilayer [2]. The study of the homologous series of alkanes is also of interest to those studying mechanisms of olfaction. Again, there are correlations between the odor of a compound and its oil-water partition coefficient [3].

Another important reason for studying the interaction of alkanes with

bilayers is due to the importance of alkanes in planar black lipid membranes. For many years black lipid membranes have been used as model membranes to study electrolyte and non-electrolyte transport [4]. Often these black lipid membranes are formed from dispersions of lipid in *n*-alkane solvents, and some of the properties of the membrane are a function of the particular *n*-alkane used [2,5—6]. It has been found from capacitance measurements that the thickness of black lipid films depends strongly on the number of carbon atoms in the *n*-alkane used as the lipid solvent [2,5—8]. Planar bilayers formed using small alkanes, containing 6—10 carbon atoms, are much thicker than those formed from longer alkanes, C12—C16 [2,5—8]. The membrane conductance of bilayers treated with certain ionophores has also been shown to be dependent on the chain length of the alkane solvent [8]. Thus, the usefulness of black lipid films as models for biological membranes may depend on the effects of the hydrocarbon solvents on the structure and properties of the bilayer [9].

Because of the importance of the interaction of bilayers with alkanes, experiments have been performed to determine the effect of the various *n*-alkanes on lipid bilayer structure and thermal properties. The *n*-alkanes, varying in length from C6 to C16, were studied in both synthetic and natural phosphatidylcholine bilayers by a combination of X-ray diffraction and differential scanning calorimetry. Surface potentials were also recorded for phosphatidylcholine monolayers containing the different alkanes.

## Materials and Methods

The *n*-alkane solvents were purchased from Applied Science or Sigma. The purity of these alkanes was given as 99% or greater, and no further purification was done. For the X-ray diffraction experiments, lipids were used as obtained from Calbiochem or Sigma. For the calorimetry experiments, the dipalmitoyl phosphatidylcholine (DPPC) was purchased from Sigma and repurified by silica gel chromatography [10]. The dimyristoyl phosphatidylcholine (DMPC) used in the monolayer and calorimetry experiments was purchased from Supelco. DPPC and DMPC were tested for purity using thin-layer chromatography [10], where each gave single spots. Double or triple distilled water was used in all experiments.

### *X-ray diffraction*

Multilamellar arrays of lipid-alkane bilayers were formed by the following procedure. Phospholipid was completely dried from chloroform solution under a gentle stream of nitrogen. The appropriate volume of *n*-alkane was then added. For some experiments, the long alkanes were simultaneously dissolved with the lipid before evaporation of the chloroform. These two techniques gave identical results. After the lipid and alkane were thoroughly mixed, water or 0.1 M NaCl adjusted to pH 7.4 was added. Identical results were obtained with water or 0.1 M NaCl. From previous X-ray diffraction studies [11—12], it is known that phosphatidylcholine is fully hydrated at about 45% water content by weight, and any additional water will form an excess water phase. Accordingly, the experiments performed in this paper were run at either of two water

concentrations: 70% water, where we were assured of having excess water in the system, and 30% water where the fluid layers between bilayers were narrower, and higher resolution X-ray diffraction patterns could be recorded. The lipid-alkane buffer suspension was then vortexed until uniform in appearance, allowed to equilibrate for 1 to 2 h in a sealed vial above the lipid transition temperature, and then transferred and sealed in quartz-glass X-ray capillary tubes. The capillaries were mounted in an X-ray camera equipped either with a point-focus collimator or a mirror-monochromator system. The X-ray generators used were a stationary anode Jarell-Ash and a rotating anode designed by Dr. William Longley of the Anatomy Department at Duke University [13]. X-ray diffraction patterns were recorded on three or more layers of Ilford Industrial G X-ray film packed in a flat-plate film cassette. Specimen-to-film distances were between 5 and 12 cm and exposure times varied from 30 min to 5 h. Discrete lamellar low-angle reflections obeyed Bragg's law, $2d \sin\theta = h\lambda$, where $d$ is the repeat period, $\theta$ is the Bragg angle, $h$ is the number of the diffraction order, and $\lambda$ is the wavelength of the incident radiation (1.54 Å). Resolution is defined as $d/h_{max}$ where $h_{max}$ is the highest diffraction order obtained. Densitometer tracers were recorded on a Joyce-Loebl microdensitometer Model MK IIIC, the background curves were subtracted, and integrated intensities $I(h)$ were measured. Electron density profiles, $\rho(x)$, were calculated by use of the formula

$$\rho(x) \propto \sum_h \phi(h)\sqrt{h^2 I(h)} \cos\frac{2\pi x h}{d}$$

where $\phi(h)$ is the phase for each order $h$, and must be + or − for these centrosymmetric systems. The correct phase combination has previously been determined for both DPPC [14] and egg phosphatidylcholine [15—16]. The phase choices for the lipid-alkane data were made by assuming a bilayer-like profile for each repeating unit. We note that the wide-angle and lamellar low-angle reflections reported in the Results section are diagnostic of bilayer phases [17]. This assumption was sufficient to determine unambiguously the phase choice for each of the orders for these relatively low-resolution data. All electron density profiles are on a relative electron density scale.

*Differential scanning calorimetry*

Differential scanning calorimetry was performed on a Perkin-Elmer DSC 1B. Thermograms were obtained in the following manner. A known amount of lipid was weighed on a modified aluminium sample pan and then a given amount of alkane was added to the lipid via a microliter syringe. The smaller alkanes appeared to wet the lipid and the lipid alkane mixture was reweighed. It is important to note that the rate of evaporation of the alkanes was significantly retarded by the lipid. For the longer alkanes, methylene chloride was sometimes added to both components to simultaneously dissolve them, although this treatment proved to be unnecessary. The solvent was subsequently removed under vacuum. The alkane concentration was determined by gas chromatography following completion of the thermogram. Twice-distilled water was rapidly added to the sample pan in a quantity to insure that the lipid was fully hydrated (usually 10 µl of water per mg lipid) and the sample pans

were then hermetically sealed. The samples were usually heated and cooled at rates from 2—5°C/min, unless otherwise specified.

*Monolayers*

The measurement of surface potential ($\Delta V$) of monolayers as a function of temperature has been described elsewhere [18]. In these experiments, 10 $\mu$l of a 12 mg/ml dispersion of DMPC in various alkane solvents (which usually contained about 5% ethanol) were deposited along the edge of a Teflon trough filled with double distilled water. This particular concentration was chosen since it is the concentration commonly used to make planar lipid bilayers. The temperature ($T$) was measured by a thermometer in the water phase and changed by flowing water through the false bottom of the Teflon chamber. The heating rate was 5°C/min. The cooling rate was not as well controlled and usually was about 8°C/min. The surface potential was measured by the ionizing electrode method [19]. We have previously shown that the thermal behavior of this system reflects the properties of a monolayer, as identical results are obtained when just enough material is added to the surface to obtain a close-packed monolayer [20]. The $\Delta V$ versus $T$ curves were cycled through the transition temperature until two consecutive runs superimposed upon each other. DMPC was chosen for the monolayer studies since the transition temperature of this lipid is closer to room temperature than that of DPPC (which was used in the X-ray and most of the calorimetry studies). This means that gradients in temperature between the gas and aqueous phases are minimized.

## Results

*X-ray diffraction*

For all alkanes, C6—C16, diffraction experiments were performed at different lipid to alkane molar ratios. For each of the lipids tested, the long spacing remained the same for dodecane, tetradecane, and hexadecane at mole fractions of 0.3—0.9. However, for the shorter alkanes, the repeat period increased as the quantity of alkane added to the bilayer was increased. For C6—C10, the repeat period increased with increasing alkane concentration until a mole fraction of between 0.6 and 0.9 was reached. The addition of more alkane did not increase the repeat period further, and thus excess alkane was present under these conditions. Since we desire information on bilayers containing the maximum amount of alkane possible, all diffraction experiments reported in this section were performed with excess alkane present in the system. These mol fractions of alkane are simply the starting mixtures in the capillary tube. We do not know the molecular ratio of lipid/alkane in the bilayers themselves. However, this information is not necessary for the interpretation of the diffraction patterns.

All diffraction patterns recorded consisted of from 2—6 lamellar orders with repeat periods ranging from 54 Å—97 Å, depending on the water content and particular alkane added to the lipid, and wide-angle reflections at 4.2 Å or 4.5 Å, depending on the physical state of the lipid.

The X-ray repeat periods for DPPC/alkane bilayers at 70% water content are

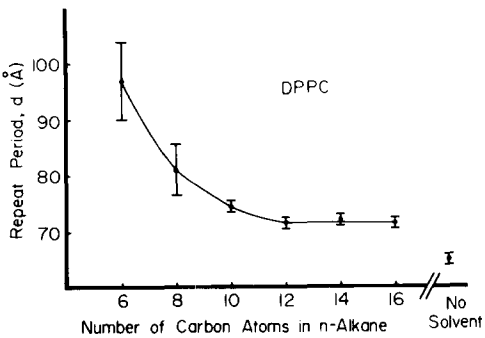


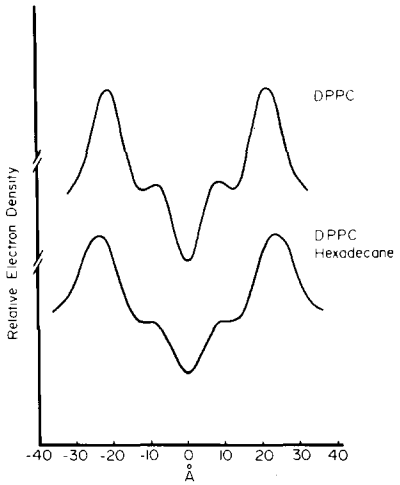


Fig. 1. X-ray repeat periods for suspensions of dipalmitoyl phosphatidylcholine (DPPC) containing excess amounts of various *n*-alkanes. The repeat period for the control, solvent-free, DPPC suspension is shown on the right side of the graph. All experiments were performed at 20°C ± 2°C, with a water content of 70%. The points represent average repeat periods of 3—6 experiments, with the error bars indicating the standard deviation.

Fig. 2. Electron density profiles for pure DPPC and DPPC with excess hexadecane, both at 70% water content.

shown in Fig. 1. Note that the repeat period is largest for DPPC with the small alkanes, but even the large alkanes (C12—C16) produce an increase in repeat period over the control pure DPPC bilayers. Pure gel state DPPC in 70% water has a repeat period of 65 Å, while this lipid mixed with dodecane, tetradecane, or hexadecane has a repeat period 6—7 Å larger. Electron density profiles at between 12 and 14 Å resolution are shown in Fig. 2. The high-density peaks centered at about ±21 Å for DPPC and at about ±24 Å for DPPC/hexadecane correspond to the phospholipid head-group, primarily the high-density phosphate group, while the low-density troughs in the center of the bilayers, at 0 Å, correspond to the lipid terminal methyl groups [14]. The relatively flat, medium-density region between the head groups and terminal methyl dip is the methylene region of the lipid hydrocarbon chains. The medium-density regions at the outside edge of each profile are the fluid spaces between bilayers. These profiles show that the width of the bilayer, as measured by head-group to head-group distance, has increased by about 6 Å upon the addition of hexadecane, while the fluid layers between bilayers have remained about the same. Notice also that the terminal methyl trough in the center of the bilayer is slightly wider and shallower when this alkane is present.

The *n*-alkanes also markedly affect the wide-angle pattern from DPPC bilayers. Pure DPPC multilayers in excess water give a sharp 4.2 Å wide-angle reflection surrounded by a diffuse broad band. This type of pattern has been interpreted in terms of a hydrocarbon chain tilt of about 30° [17]. X-ray patterns of oriented hydrated multilayers of DPPC show this chain tilt directly [21—22]. However, the wide-angle pattern of DPPC with any of the *n*-alkanes consists of a single sharp band at 4.2 Å, indicative of untilted hydrocarbon

chains [17,23]. Thus, the *n*-alkanes remove the chain tilt and this causes an increase in the bilayer width. For the long alkanes, the increase in bilayer width of about 6 Å can be fully accounted for by this loss of chain tilt since (48 Å) cos 30° ≅ 42 Å. However, for the shorter alkanes, the repeat periods are much longer than can be accounted for by two fully extended DPPC molecules plus the water spaces between bilayers. For example, the average DPPC/hexane repeat period of 97 Å is a full 32 Å longer than the control pure DPPC repeat. Only 3 and 2 orders of diffraction could be recorded from DPPC/octane and DPPC/hexane specimens respectively, and electron density profiles were not computed.

The long spacings for two lipids, dilauroyl phosphatidylcholine (DLPC) and egg phosphatidylcholine, in the liquid crystalline state mixed with the *n*-alkanes in excess water are shown in Fig. 3. In all of these experiments, the wide-angle diffraction pattern consisted of a broad reflection at 4.5 Å, characteristic of the liquid-crystalline state [15,17]. For both lipids, the curves of Fig. 3 have similar characteristics, with the shorter alkanes increasing the lipid repeat periods to a much greater extent that the long alkanes. For both DLPC and egg phosphatidylcholine, the bilayers with added hexadecane have the same repeat period as the control, alkane-free bilayers, 59 Å for DLPC and 63 Å for egg phosphatidylcholine. For DLPC, the repeat period is approximately constant for alkanes C16—C10, whereas much larger repeat periods are recorded for C6 and C8. For egg phosphatidylcholine, the large increase in repeat period begins with C12. In other words, the 'cut-off' point for large increase in repeat periods comes at different lengths of incorporated alkanes in DLPC than for egg phosphatidylcholine. Except near the cut-off point of DLPC at C10, the two curves are separated by a uniform distance of about 5 Å.

The longer alkanes have a smaller effect on the repeat periods of DLPC and egg phosphatidylcholine than on DPPC (Fig. 1). This probably occurs because the

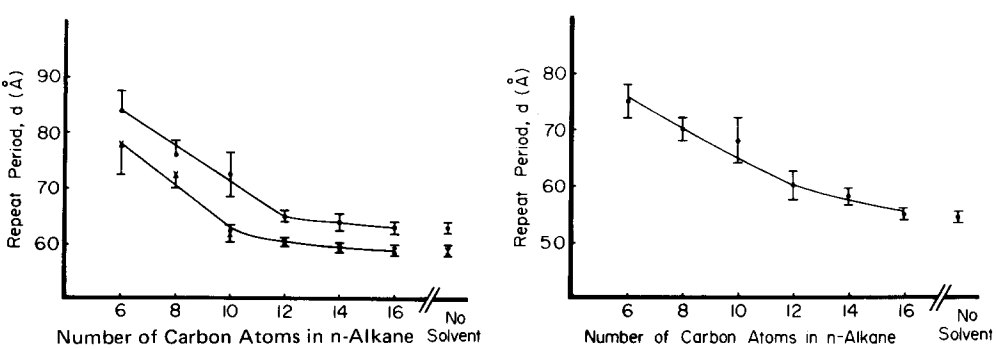


**Fig. 3. Repeat periods for suspensions of egg phosphatidylcholine (•) and dilauroyl phosphatidylcholine (DLPC) (X) containing various *n*-alkanes at a mole fraction of alkane of 0.6. The repeat periods for the solvent-free lipids are shown on the right side of the graph. All experiments were performed at 20 ± 2° C, with a water content of 70%. The points represent average repeat periods of 2—5 experiments, with the error bars indicating the standard deviation.**

**Fig. 4. Repeat periods for suspensions of egg phosphatidylcholine excess alkane at 30% water content at 20 ± 2° C. The points represent average repeat periods of 2—5 experiments, with the error bars indicating the standard deviation.**

lipid hydrocarbon chains are not in a tilted configuration in the liquid-crystalline state. As a matter of fact, in the case of fully hydrated egg phosphatidylcholine, the addition of tetradecane and hexadecane does not increase the repeat period within experimental error. However, these longer alkanes do have one effect, namely to improve the resolution of the diffraction patterns. Fully hydrated egg phosphatidylcholine gives two or three reflections, while patterns from egg phosphatidylcholine/tetradecane and egg phosphatidylcholine/hexadecane contain four diffraction orders under the same experimental conditions. The patterns for egg phosphatidylcholine/hexane and egg phosphatidylcholine/octane at 70% water content also only contain two diffraction orders.

To improve the resolution, additional experiments were performed at reduced (30%) water content. Fig. 4 shows the long spacing for egg phosphatidylcholine/alkane preparations at 30% water content. The curve has a similar shape to the graph of egg phosphatidylcholine/alkane at 70% water (Fig. 3), except that the entire 30% curve is shifted downward by about 7 Å. This is because the bilayer is about 3 Å wider although the fluid layer between bilayers is about 10 Å narrower for egg phosphatidylcholine at 30% hydration compared to egg phosphatidylcholine at 70% hydration [11]. Fig. 5 shows electron density profiles for egg phosphatidylcholine with various alkanes. The egg phosphatidylcholine/hexadecane profile shows a sharpened terminal methyl trough in the center of the bilayer as compared to pure egg phosphatidylcholine. However, as the length of the *n*-alkane decreases, the bilayer width increases and the terminal methyl dip becomes broader and shallower. In the egg phosphatidylcholine/hexane profile the width has increased to about 53 Å, and the terminal methyl trough has almost completely vanished. The terminal methyl trough diminishes primarily because of changes in the intensity distribution in the diffraction patterns (Table I), and not because of the differences in resolution in the series of profiles of Fig. 5.

*Differential scanning calorimetry*

Fig. 6 shows thermograms for DPPC without any organic solvents (curve A) and DPPC with the following mole fractions of alkane: (B) 0.98 hexane; (C) 0.98 octane; (D) 0.96 decane; (E) 0.29 decane; (F) 0.96 dodecane; and (G) 0.95 tetradecane. The numbers represent the mole fraction of alkane in the sample pan. They do not represent the amount of alkane solubilized in the bilayer. Clearly there is excess alkane in certain cases and probably some

TABLE I

STRUCTURE AMPLITUDE ($\sqrt{h^2 I(h)}$) DATA

| *h* | Egg phosphatidylcholine *d* = 53 Å | Egg phosphatidylcholine/Hexadecane *d* = 54 Å | Egg phosphatidylcholine/Decane *d* = 63 Å | Egg phosphatidylcholine/Octane *d* = 68 Å | Egg phosphatidylcholine/Hexane *d* = 74 Å |
|---|---|---|---|---|---|
| 1 | 1.00 | 1.00 | 1.00 | 1.00 | 1.00 |
| 2 | 0.32 | 0.04 | ≃0 | 0.16 | 0.21 |
| 3 | 0.34 | 0.23 | 0.31 | 0.59 | 0.46 |
| 4 | 0.24 | 0.35 | 0.42 | 0.50 | 0.22 |

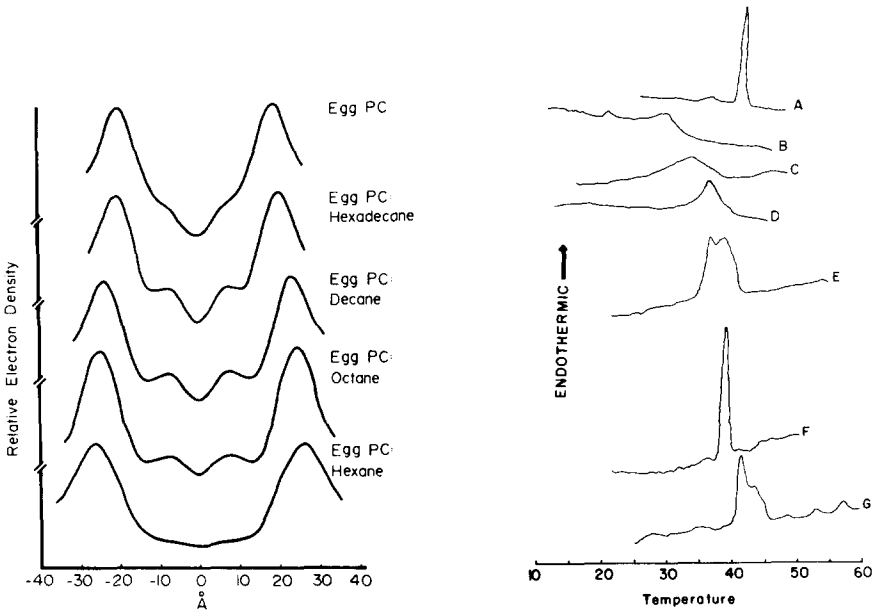


Fig. 5. Electron density profiles for suspensions of egg phosphatidylcholine (Egg PC) containing excess alkane at 30% water content.

Fig. 6. Thermograms for DPPC in excess water without any organic solvents (A) and DPPC with the following mole fractions of alkane: (B) 0.98 hexane; (C) 0.98 octane; (D) 0.96 decane; (E) 0.29 decane; (F) 0.96 dodecane; and (G) 0.95 tetradecane. Since the concentrations of lipid and sensitivities were different for these different thermograms, the relative areas under the curves are not representative of the relative enthalpies. The enthalpies are given in the text. The samples were scanned at both 5 and 10°C/min rates and the arrow indicates the direction of heat flow.

monolayer covered oil drops are present. The concentrations in B—D, F, and G were chosen to insure that there was excess solvent in the system.

The control thermogram for DPPC (A) has values for the transition parameters that are in general agreement with those reported by others [24]. The main endothermic transition at 41°C is sharp, and the broader pretransition peak has its maximum at 35°C. The addition of excess hexane (B) greatly broadens the main endothermic peak, reduces the transition temperature to 29°C, and reduces its enthalpy by 88% to about 1 kcal/mol. Furthermore, a new thermal event appears at 20°C. When the alkane mole fraction was reduced to 0.36, these two peaks remained constant in shape with the main peak having an enthalpy of transition of about 4 kcal/mol (data not shown). From C, it is clear that octane behaves in a similar fashion to hexane, except that the main transition occurs at 32.5°C and has an enthalpy of 4.3 kcal/mol. No other peaks are evident.

Upon the incorporation of decane (D), the pretransition peak disappears and a single broad peak appears at 36°C with an enthalpy of 6.5 kcal/mol. However, this single peak is actually comprised of two peaks which can be seen in the cooling curve (not shown). These two peaks can be more easily seen during heating if the lipid-alkane mol ratio is increased (E). Here two peaks appear at 36°C and at 39°C. When dodecane is incorporated into the bilayer (F)

the main endothermic transition is relatively sharp. The dispersion melts at 38°C and has an enthalpy about the same as the control. The pretransition peak has obviously disappeared. When tetradecane is the solvent (G), two main transitions are evident, one at 42°C and the other at 44°C. The enthalpy, as calculated from the total area under both major peaks, is the same as that of the control, whereas that under the first peak is about 6 kcal/mol, or about 70% of the total enthalpy.

The phase diagram of DPPC with *n*-hexadecane is seen in Fig. 7. The line connecting the closed circles (●) is the peak of the endothermic transition upon heating. The vertical bars through these points represent the width of the transition at half height. There was evidence of two peaks at mol fractions $X_{HD}$ = 0.075 and 0.10. However, these were obvious only on cooling curves. At mol fractions of 0.03, 0.14, and 0.21, there was a single peak both on heating and cooling. The relative enthalpy of the main endothermic transition is seen by the curve connecting the open circles. The relative enthalpy does not change from the control to a mol fraction of 0.025 where it increases, as does the transition temperature, until a mol fraction of 0.14 is reached, whereupon it remains constant. The dashed line connecting the X's is the relative enthalpy of the *n*-hexadecane peak. The first appearance of this event occurred at a mol fraction of 0.14, the point where the transition temperature and enthalpy became independent of the *n*-hexadecane concentration. If we take the amount of hexadecane incorporated into the bilayer to be maximally $X_{HD}$ = 0.1, then the volume fraction of hexadecane in the DPPC is about 5%.

Fig. 8 shows a graph of the transition temperature of DPPC (highest main

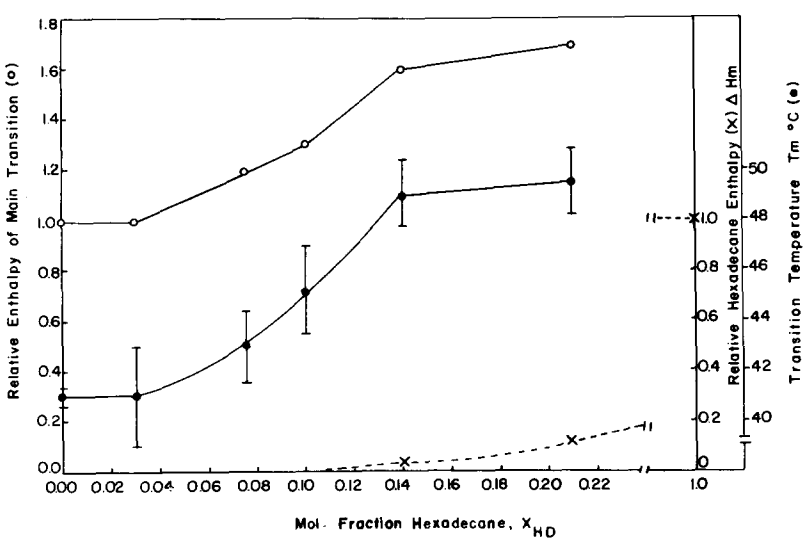


Fig. 7. Graph of the relative enthalpy (as compared to the pure component) of the main endothermic transition of DPPC/hexadecane suspensions (○) and hexadecane (X), and the transition temperature of the main endothermic transition (●) as a function of mole fraction of hexadecane in the sample ($X_{HD}$). The vertical bars through the solid circles (●) represent the peak width at half height of the main transition. The dotted line extrapolates to zero for $0.10 < X_{HD} < 0.14$. This zero point represents the mole fraction of hexadecane solubilized in the gel phase of DPPC. The heating rates were varied between 2.5 and 50°C/min.

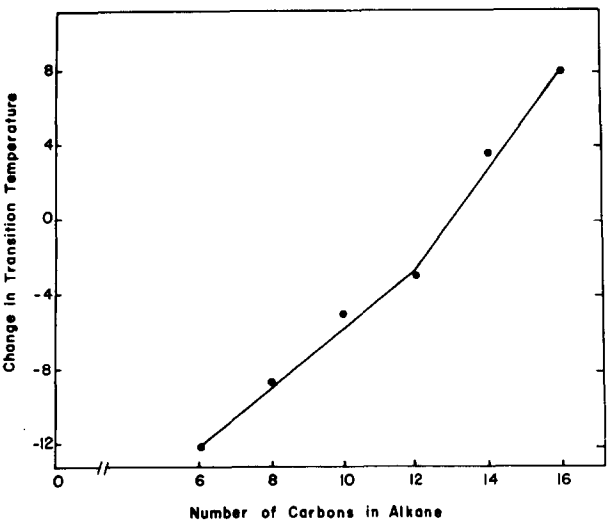


Fig. 8. The transition temperature of the main endothermic peak for DPPC/alkane suspensions as a function of number of carbon atoms in the alkane, as taken from the thermograms of Figs. 6 and 7.

endothermic peak) with excess alkane present as a function of the number of carbons in the alkane. The data in this figure were obtained from Figs. 6 and 7. It is of interest that the break in the curve occurs at dodecane (C12), a position corresponding to the change in slope of the curve of Fig. 1.

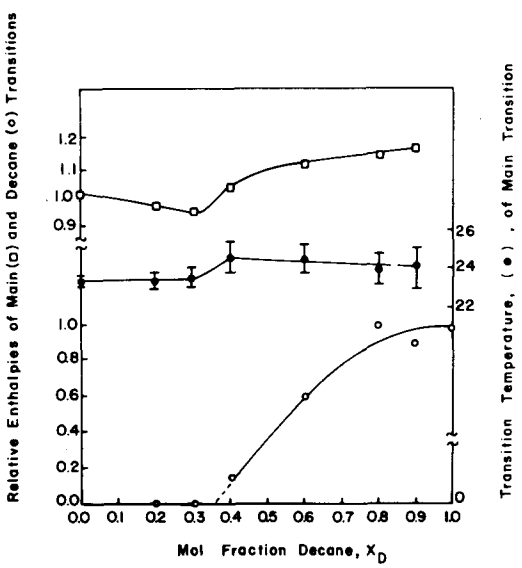


Fig. 9. Graph of the relative enthalpy (as compared to the pure component) of the main endothermic transition of dimyristoyl phosphatidylcholine (DMPC)/decane suspensions (□) and decane (○), and the transition temperature of the main endothermic transition (●) as a function of the mole fraction of decane in the sample ($X_D$). The bars through the solid circles (●) represent the peak width at half height of the main transition. The dotted line extrapolates to zero at $X_D \tilde{=} 0.35$. This point represents the mole fraction of decane solubilized in the gel phase of DMPC. The samples were heated and cooled several times at rates between 2.5 and 10° C/min.

Fig. 9 shows the phase diagram for DMPC/decane in excess water. The transition temperature of the main endothermic transition (●), the relative enthalpy of the main endothermic transition of DMPC/decane (□), and the relative enthalpy of the decane transition (○) as a function of mol fraction of *n*-decane in the sample are shown. Abrupt changes in each of the curves occur at a mol fraction of 0.4. At mol fractions less than 0.3 the transition temperature remains unchanged, whereas the enthalpy of the transition slightly decreases and the decane peak is not evident. At mol fractions of decane greater than 0.4, the transition temperature remains constant whereas the relative enthalpy of the lipid decane dispersion and the enthalpy of the decane increase, the former much more slowly than the latter. At a mol fraction of decane of 0.4, two peaks were observed in the cooling curve, although only one was observed in the heating curve. At all other mol fractions only a single peak was observed in both heating and cooling curves (Fig. 10C). Upon extrapolation, the zero of the curve of relative enthalpy of decane enthalpy would occur at a mol fraction of 0.35, which corresponds to a mol ratio of lipid to decane of 1.9 : 1. Thus decane would occupy a volume fraction of about 16% in the gel phase of DMPC.

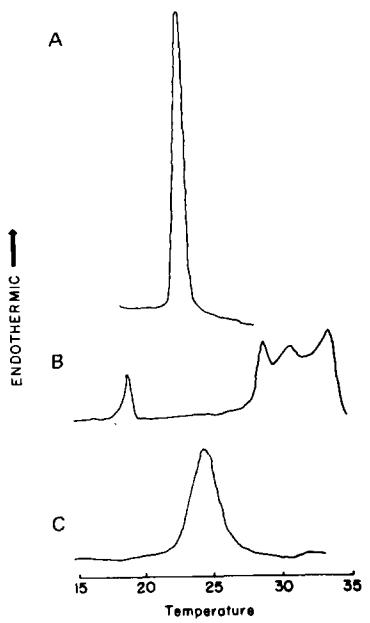


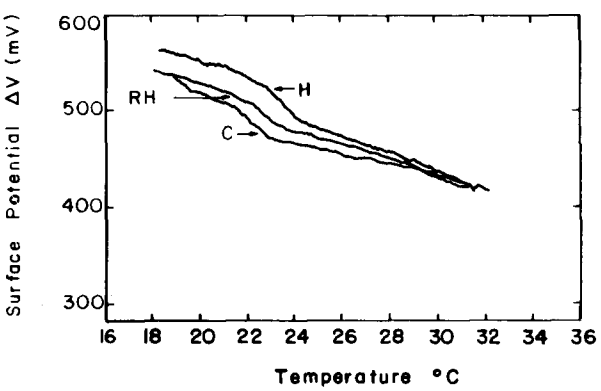


Fig. 10. Thermograms for DMPC in excess water without any organic solvents (A) and DMPC with 0.3 mol fraction hexadecane (B) and with 0.3 mol fraction decane (C). Notice in curve (B) the peak at 18°C represents a pure hexadecane transition, indicating that there is excess hexadecane not solubilized in the bilayer. The arrow indicates the direction of heat flow. The samples were scanned at rates between 2.5 and 50°C/min with essentially identical results.

Fig. 11. The surface potential of DMPC as a function of temperature. The DMPC was spread at 18.4°C using a 12 mg/ml concentration of lipid in methanol. The curve labeled H was the first heating curve, which is not reproduced on successive heating cycles. The curves labeled C and RH are cooling and reheating curves. Both the C and RH curves are reproducible upon subsequent temperature cycles. The transition temperature (23°C) is the point on the RH curve where the curve levels off and the slope remains constant.

Fig. 10 shows thermograms for (A) pure DMPC; (B) DMPC/hexadecane at a mol fraction of hexadecane of 0.3; and (C) DMPC/decane at a mol fraction of decane of 0.3. The pure DMPC has a sharp transition at 23.5°C, while both hexadecane and decane modify the thermogram. At this concentration of hexadecane, there is clearly a separate phase of hexadecane, which melts at 18°C. There are also three thermal events at temperatures higher than the pure DMPC transition. In the case of DMPC/decane, there is one peak which is broader and at a slightly elevated temperature compared to the control.

*Surface potential*

The change in surface potential with temperature of a monolayer of DMPC is shown in Fig. 11. The monolayer was spread from a methanol solution at 18.4°C. This figure illustrates several points that are common to this type of measurement. If the monolayer is spread below the transition temperature of the lipid, the first heating curve will usually not be reproduced on subsequent heating cycles. The first heating curve has a higher melting temperaure than subsequent heating cycles, which are reproducible. The second heating (labeled RH) generally yields a lower surface potential than the first heating. The transition temperature is defined arbitrarily at the abrupt end of the surface potential drop in the RH curve. In Fig. 11 the transition temperature is 23°C. As seen in Fig. 11, there is a hysteresis loop between the reproducible heating (RH) and cooling (C) curves. Nevertheless, for temperatures well above and below the transition temperatures, the surface potential for these two curves is the same. If the monolayer is spread above its transition temperature, no metastable states are produced and all the heating curves can be superimposed. Results similar to those of Fig. 11 are obtained when DMPC is spread from

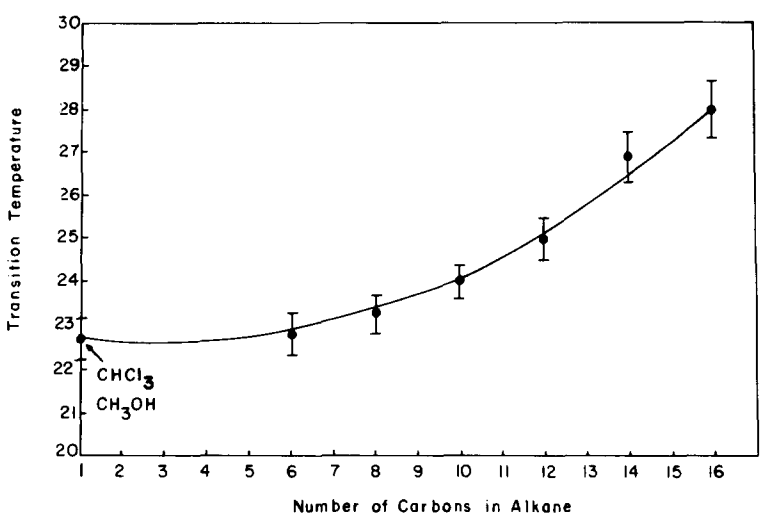


Fig. 12. The transition temperature of the reheating (RH) curve of monolayers as a function of the number of carbon atoms in the spreading solvent. The control values, shown on the left vertical axis, were obtained using chloroform ($CHCl_3$) and methanol ($CH_3OH$) as spreading solvents. Both chloroform and methanol quickly evaporate from the surface. The points represent the mean values and the error bars represent the standard error of the mean.

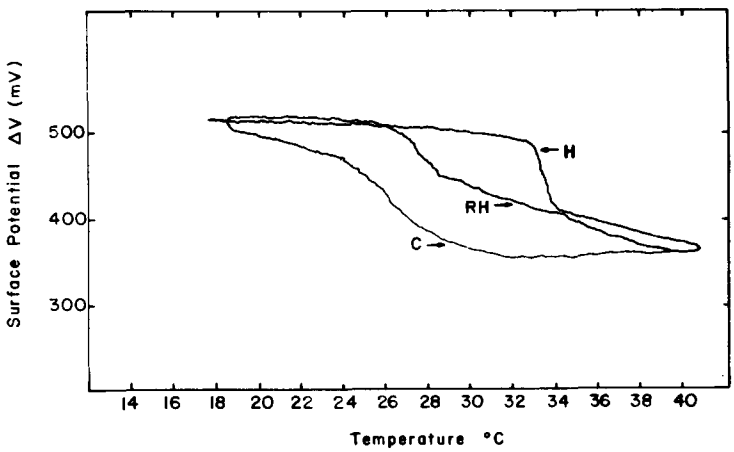


Fig. 13. The surface potential of a DMPC monolayer with hexadecane as the spreading solvent as a function of temperature. The monolayer was spread at 19°C, which is above the melting-point of hexadecane but below the melting temperature of DMPC. The curve H represents the first heating curve, which is not reproducible, while C and RH represent the reproducible cooling and reheating curves, respectively.

chloroform or *n*-hexane (Fig. 12). Both of these solvents evaporate from the surface, if they did not they would lower the transition temperature as was found by calorimetry (Fig. 6). Similar arguments may also be applicable to octane. It is clear, however, that the longer alkanes do indeed interact with the monolayer in a manner that increases the transition temperature. This is true even if the alkane is longer than the length of the lipids, as is the case for *n*-hexadecane in DMPC. This behavior is best seen in Fig. 13 in which DMPC was spread with *n*-hexadecane, at 19°C, a temperature which is above the hexadecane transition temperature but below the lipid transition. The transition on the first heating curve (H) occurs at about 33°C over a very narrow temperature range. The second heating curve (RH) again has a lower melting temperature with its transition at 28°C. Notice also that the surface potential is lower in hexadecane-containing membranes than membranes without appreciable amounts of solvents. The width of the transition is considerably broader, as it is in the calorimetry data (Fig. 10).

Fig. 12 shows how the transition temperature of DMPC monolayers changes with increasing chain length of the spreading solvent. The transition temperatures represent the end of the transition for the reproducible heating (RH) curves. Note that the transition temperature does not significantly change until decane, a solvent that only slowly evaporates from the surface, is used. We observed that for monolayers spread with alkanes smaller than decane, the solvents appear to wet the monolayer, as few lenses are seen. In contrast, when alkanes of the size of decane and larger are used to spread the monolayer, lenses are evident and the alkanes do not appear to wet the monolayer.

## Discussion

### *Localization of the alkanes in the bilayer*

These results show that all the *n*-alkanes tested, from C6—C16, enter the

hydrocarbon region of phosphatidylcholine multilayers, in both the gel and liquid crystalline states, for both saturated (DPPC) and unsaturated (egg phosphatidylcholine) lipids. The evidence that these alkanes entered saturated gel state lipids is that they all modify the wide-angle and lamellar X-ray diffraction patterns. The longer alkanes (C12—C16) increase the bilayer width by an amount consistent with the reduction in chain tilt from approx. 30—0°. Electron density profiles (Fig. 2) show that this increase in repeat periods is indeed due to an increase in bilayer width. The profiles also show that, although the long alkanes broaden the terminal methyl trough somewhat, there is still a distinct electron density trough in the center of the bilayer. These data strongly suggest that the longer alkanes align themselves parallel to the lipid hydrocarbon chains. thus effecting hydrocarbon chain packing and chain tilt, but not increasing bilayer width beyond the length of two fully extended DPPC molecules. The apparent reason the alkanes remove chain tilt is because they lie between the lipid acyl chains and decrease the projected area per lipid molecule [25].

Like the long alkanes, the short alkanes must intercalate between acyl chains of the bilayer. This has been noted in previous papers [5,26—27] and is demonstrated by the change in wide-angle diffraction, as well as by the reduction in the transition temperature and the increased peak width of the transition (Fig. 6) caused by hexane and octane in DPPC bilayers. The broadening of the peaks in the thermograms (Fig. 6) shows that there is a decrease in cooperativity between the acyl chains. However, unlike the long alkanes, the short alkanes also appear to form a separate alkane phase, almost certainly in the geometric center of the bilayer. From space filling models, the phosphate group separation across a DPPC bilayer with two fully extended lipid chains, with no chain tilt, is about 48 Å. This is precisely the head-group separation in the DPPC/hexadecane profile of Fig. 2. Thus, the DPPC/hexadecane repeat period of 71 Å corresponds to the fully extended bilayer and fluid space between bilayers. DPPC/hexane has a repeat period of 97 Å. In the case of DPPC/hexane, the resolution of the DPPC/hexane data is too low to calculate an electron density profile. However, since the alkane solubilities in water are very low, we see no reason why hexane should affect the fluid spaces between bilayers differently than hexadecane. Therefore, the 26 Å difference in repeat period for DPPC/hexane and DPPC/hexadecane is apparently due to a region of hexane between apposing lipid monolayers.

For lipids above the phase transition temperature, the results are somewhat similar. For fully hydrated bilayers (Fig. 3), the long alkanes have little effect on repeat period, while the short alkanes increase the average long spacing by as much as 21 Å over the control, as in the case of egg phosphatidylcholine/hexane. For partially hydrated egg phosphatidylcholine (30% water content), electron density profiles clearly show the effect of the alkanes (Fig. 5). The long chain hexadecane increases the depth of the terminal methyl dip compared to pure egg phosphatidylcholine, indicating that hexadecane tends to localize the terminal methyl groups of the lipids in the center of the bilayer. The most likely explanation for this phenomenon is that hexadecane enters the bilayer and lies approximately parallel to the lipid hydrocarbon chains, thereby straightening the chains and reducing the number of kinks or *gauche* conforma-

tions. Profiles of egg phosphatidylcholine/octane and egg phosphatidylcholine/hexane (Fig. 5) show a broader bilayer, with no terminal methyl dip remaining in the case of hexane. Since the average density of hexane is closer to the density of lipid methylene groups than methyl groups, these profiles strongly suggest that there is a region of hexane located in the center of the bilayer.

*Comparison of X-ray and capacitance data*

It is of interest to compare these X-ray diffraction results with calculations of bilayer widths made from electrical studies of black lipid membranes. Capacitance measurements of egg phosphatidylcholine bilayers formed from the various *n*-alkanes have been made by Haydon et al. [2] and are shown by the solid line in Fig. 14. Comparisons between the X-ray and capacitance data involve a number of assumptions. Capacitance data provide a 'hydrocarbon thickness', provided the dielectric constant of the bilayer is known. X-ray repeat periods, on the other hand, give the total thickness of the unit cell, which includes the fluid layer between bilayers and the entire bilayer-lipid head group as well as the hydrocarbon chain region. Further analysis is needed to determine the hydrocarbon region from the X-ray data. We use two methods to do this. In the first method, we estimate the hydrocarbon thickness directly from the Fourier syntheses of Fig. 5. We assume that the structural differences between fully hydrated and partially hydrated (30% water content) bilayers are small. Previous X-ray diffraction studies [11,28—29] indicate the difference in thickness between fully and partially hydrated egg phosphatidylcholine bilayers is less than 3 Å. We also assume that the 'hydrocarbon layer' thickness extends from carbonyl-group to carbonyl-group across the bilayers. To obtain the hydrocarbon layer thickness from the Fourier syntheses, we first measured the separation between head group peaks in the profiles of Fig. 5. We then used the neutron diffraction data of Buldt et al. [30] to get an accurate estimate of the distance between the high density phosphate group and the carbonyl group. Using these values, a carbonyl to carbonyl separation was obtained for egg phosphatidylcholine bilayers and egg phosphatidylcholine with each of the

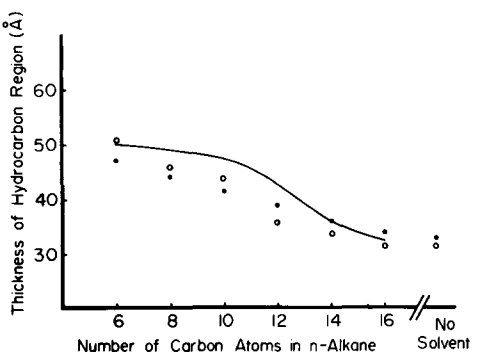


Fig. 14. Comparisons of hydrocarbon region thickness for egg phosphatidylcholine containing excess alkane as computed from capacitance and X-ray diffraction data. Capacitance data (———) were from the work of Haydon et al. [2] on planar black lipid membranes, while the X-ray thicknesses were obtained either from the electron density profiles of Fig. 5 (●), or by subtracting the fluid layers obtained by Small [11] from the X-ray repeat periods of Fig. 4 (○). The hydrocarbon thickness has been calculated for the solvent-free bilayers by both X-ray procedures and is shown on the right hand side of the graph. No capacitance data are available for solvent-free egg phosphatidylcholine bilayers.

alkanes. These numbers are shown as closed circles in Fig. 14. Note that these values are similar to capacitance results, especially for the long alkanes where the agreement is excellent. For the shorter alkanes, the resolution of the electron density profiles is reduced, so the estimates of the head group separations are less accurate. The second method of estimating hydrocarbon thickness from the X-ray data is to take the repeat periods of Figs. 3 and 4, and subtract the values of the thickness of the fluid and head group layers for these hydrations as calculated by Lecuyer and Dervichian [28], Small [11], or LeNeveu et al. [29]. The estimates of fluid-head group thickness vary by a small amount for these studies, and we chose to use the values of Small [11] because his value for the alkane-free egg phosphatidylcholine hydrocarbon width at 30% water content is closest to our value as calculated from electron density profiles (Fig. 14). Taking Small's value for fluid-head group thickness at 30% hydration and subtracting this from the repeat periods of Fig. 4 gives the open circles shown in Fig. 14 (LeNeveu's value of fluid width would give values 8 Å larger). The same sort of analysis has been done for the 70% hydration data in Fig. 3, but is not included in Fig. 14 to avoid confusion. In the 70% hydration case, LeNeveu et al.'s value for the fluid layers gives the closest match to the capacitance results. Clearly, there is some uncertainty in these calculations of fluid widths, and moreover, this method assumes that the fluid layer does not change thickness as alkane is added to the bilayer.

Given all the assumptions involved in making the comparisons of Fig. 14, the capacitance and X-ray results are quite similar. The largest mismatch between the closed circles and the capacitance results is only 5 Å. There are several possible reasons for the small mismatch between the X-ray and capacitance results. In addition to the difficulties in obtaining hydrocarbon thickness from the X-ray diffraction data, there are many uncertainties in calculating hydrocarbon thickness from capacitance data, which have been discussed by others [5,7]. Other important considerations are the differences in geometry and boundary conditions between multiwalled vesicles and planar black lipid bilayers [9].

*Calorimetry*

From Figs. 6 and 8 it is clear that there is a change in the manner in which alkanes interact with bilayers when the chain length of the alkane is more than four methylene groups shorter than the length of the acyl chains of the lipid. The importance of this factor of four methylene groups difference between the lipid and solute has been previously noted for the fatty acids in DPPC [24,31]. In the case of DPPC, alkanes shorter than dodecane (C12) lower the transition temperature and enthalpy of the main endothermic transition, as well as greatly broaden the transition. In contrast, tetradecane and hexadecane increase the transition temperature and enthalpy of the main endothermic transition. The peak width is also sharper with these long alkanes than with the shorter ones. Hunt and Tipping [27], using NMR techniques, found similar results for sonicated DPPC vesicles containing decane and hexadecane. It is pertinent that this change in the characteristics of the transition occurs at dodecane (Figs. 6 and 8), which is the cut-off point where the X-ray repeat period becomes independent of the length of the alkane (from C12 to C16, see Fig. 1).

The reason that the transition temperature of DPPC increases when hexadecane or tetradecane molecules are intercalated between the chains is apparently due to the resulting increase in hydrocarbon chain interaction. Jähnig et al. [32] have shown that for dihexadecylphosphatidic acid the phase transition temperature increases as chain tilt decreases. The short alkanes lower and broaden the DPPC transition, as the lipid acyl chains apparently become more disordered to accomodate them. This disordering decreases the van der Waal's interactions, which are primarily responsible for determining the phase transition temperature [33]. Such disordering would account for the lower resolution of diffraction patterns recorded from DPPC/hexane and DPPC/octane as compared to pure DPPC or DPPC/hexadecane. The reduction in van der Waal's interactions caused by small alkanes is also evident from monolayer studies of saturated lipids at the oil-water interface [34].

When the alkanes are mixed in excess with DPPC one to three major peaks are observed. This suggests the presence of a corresponding number of phases. For hexane and octane, where the alkane molecules are located between apposing monolayers as well as between lipid acyl chains, only one peak is observed (with the exception of a small anomalous peak at 20° in the case of hexane). For octane and hexane it is likely that all lipid molecules are in contact with alkane. For the longer alkanes, decane to hexadecane, two phases may exist, perhaps with different stoichiometries. The idea that the two peaks in the thermograms correspond to an alkane-lipid phase and an almost solvent-free phase is supported by the data from DPPC with different amounts of decane. At a mole fraction of decane of 0.29 there are two distinct peaks in the heating curve (Fig. 6E), while at a mole fraction of 0.96 there is only one peak (Fig. 6D). For the longer alkanes which are positioned parallel to the lipid acyl chains and occupy as little as 5% of the volume of the bilayer (in the case of hexadecane in DPPC), there is not enough alkane present to contact all the lipid molecules. The thermograms of tetradecane (Fig. 6G) and hexadecane (not shown) in DPPC resemble the melting behavior of two partially miscible lipids [35]. The DPPC molecules in contact with tetradecane or hexadecane act as a higher transition temperature component [36]. In the special case where the alkane chain length is four carbons smaller than the length of the lipid, the transition temperature and width remain relatively unchanged (Figs. 6F and 10C). When the chain length of the alkane is greater than the length of the lipid, as in the case of hexadecane in DMPC, three major peaks are observed (Fig. 10B). The origin of the third peak is unknown, although it may represent a monolayer covered lens (see monolayer discussion).

Because hexadecane has the lowest vapor pressure and highest melting-point (18°C) of the alkanes we investigated, its effect on the transition parameters of DPPC was studied in greater detail than most of the other alkanes. Extrapolation of the enthalpy of the hexadecane transition to zero (Fig. 7) reveals that at a mol fraction of hexadecane in the bilayer of between 0.10 and 0.14 a separate hexadecane phase appears. Thus the amount of hexadecane that can be solubilized in the bilayer below its transition temperature is between 0.10 and 0.14 mol fraction of hexadecane, or one hexadecane molecule per 6—10 lipid molecules. For comparison, we note that palmitic acid can be incorporated into DPPC bilayers at a mol fraction of 0.67 [24,31]. Since hexadecane is

aligned parallel to the lipid acyl chains, the exposure of methyl groups of the alkane to water at the lipid head group region is probably a major factor in limiting the solubility of hexadecane in bilayers.

*Behavior of monolayers*

Under appropriate conditions, monolayers of saturated lecithins at the air-water interface are good models for half a bilayer [33]. Thus, we have used different solvents to spread monolayers at the air-water interface to determine if these different solvents affect the properties of monolayers in a similar manner to the way they affect bilayers. This type of approach has been successful in the past [20]. Fig. 12 shows that monolayers spread from chloroform or methanol have the same transition temperature as those spread from hexane or octane. The transition temperature of the DMPC monolayer remained unchanged at 23°C. The obvious interpretation is that these volatile solvents evaporated during the spreading and heating of the monolayer. We note that in bilayers, where evaporation is prevented, chloroform, methanol [34,37], and hexane and octane (Fig. 6) reduce the phase transition temperature.

For the longer alkanes, that do not evaporate during the course of the experiment, the transition temperature of the monolayer increases with chain length, from C10 to C16 (Fig. 12). A comparison of the data of Fig. 12 with the calorimetry data of DMPC in Fig. 10, provides a direct correlation between the effect of alkanes on monolayers and bilayers. For DMPC/hexadecane bilayers (Fig. 10B), the occurrence of three thermal events, all at higher temperatures than the control, shows that hexadecane does indeed increase the transition temperature and have multiple transitions. The highest peak in this thermogram occurs at the same temperature as the transition in the first heating curve (H) of the monolayer. The peak at 28°C in the thermogram (Fig. 10B) corresponds to the reproducible monolayer transition (RH in Fig. 13). A mol fraction of hexadecane of 0.3 was chosen for the calorimetry scan to ensure that there was excess alkane in the system, and indeed a separate hexadecane phase at 18°C is noted in the thermogram of Fig. 10B. The DMPC/decane thermogram (Fig. 10C) is very similar to the monolayer data (Fig. 12), in that there is only one peak, which is broader and at a slightly higher temperature than the control.

Thus, the X-ray, calorimetry, and monolayer data all show that long and short alkanes interact in different manners with phosphatidylcholine bilayers. In the past, X-ray diffraction experiments have provided information on the solubility of alkanes in micelles and smectic phases [38]. Since the thicknesses of planar bilayers (Fig. 14) and the repeat periods for multiwalled vesicles (Figs. 1 and 3) and micelles [38] all have similar behavior as a function of the chain length of the incorporated alkane, it seems likely that the laws which govern solubility of alkanes are similar for these three systems.

**Acknowledgements**

We wish to thank Mrs. Pat Thompson for an excellent job in typing this manuscript. This work was supported by National Institutes of Health Grants 9 P01 GM 23911 and HL 12157 and ONR Contract N00014-A-0251-0022.

## References


1 Carter, D.E., and Fernando, Q. (1979) J. Chem. Edu. 56, 284—288
2 Haydon, D.A., Hendry, B.M., Levinson, S.R. and Requena, J. (1977) Biochim. Biophys. Acta 470, 17—34
3 Patte, F., Etcheto, M. and Laffort, P. (1975) Chem. Senses Flavor 1, 283—325
4 Tien, H.T. (1974) Bilayer Lipid Membranes, Theory and Practice, Marcel Dekker, New York
5 White, S.H. (1977) Ann N.Y. Acad. Sci. 303, 243—265
6 Benz, R., Fröhlich, O., Läuger, P. and Montal, M. (1975) Biochim. Biophys. Acta 394, 323—334
7 Fettiplace, R., Andrews, D.M. and Haydon, D.A. (1971) J. Membrane Biol. 5, 277—296
8 Hendry, B.M., Urban, B.W. and Haydon, D.A. (1978) Biochim. Biophys. Acta 513, 106—116
9 Ebihara, L., Hall, J.E., MacDonald, R.C., McIntosh, T.J. and Simon, S.A. (1979) Biophys. J. 28, 185—196
10 Kates, M. (1972) in Laboratory Techniques in Biochemistry and Molecular Biology (Work, T.S. and Work, E.), Part II, pp. 393—469, North-Holland Publishing Co, Amsterdam
11 Small, D.M. (1967) J. Lipid Res. 8, 551—557
12 Janiak, M.J., Small, D.M. and G.G. Shipley (1976) Biochemistry 15, 4574—4580
13 Longley, W. and Miller, R. (1975) Rev. Sci. Instrum. 46, 30—32
14 Lesslauer, W., Cain, J.E. and Blasie, J.K. (1972) Proc. Natl. Acad. Sci. U.S.A. 69, 1499—1503
15 Levine, Y.K. and Wilkins, M.H.F. (1971) Nature 230, 69—72
16 Torbet, J. and Wilkins, M.H.F. (1976) J. Theor. Biol. 62, 447—458
17 Tardieu, A., Luzzati, V. and Reman, F.C. (1973) J. Mol. Biol. 75, 711—733
18 MacDonald, R.C. and Bangham, A.D. (1972) J. Membrane Biol. 7, 29—53
19 Gaines, G. (1966) Insoluble Monolayers at Liquid-Gas Interfaces, Chapter 2, Interscience, New York
20 Simon, S.A., Lis, L.J., MacDonald, R.C. and Kauffman, J.W. (1975) Biochim. Biophys. Acta 375, 317—326
21 Levine, Y.K. (1973) Surf. Sci. 3, 279—352
22 McIntosh, T.J. (1978) Biochim. Biophys. Acta 513, 43—58
23 Brady, G.W. and Fein, D.E. (1977) Biochim. Biophys. Acta 464, 249—259
24 Mabrey, S. and Sturtevant, J.M. (1977) Biochim. Biophys. Acta 486, 444—450
25 McIntosh, T.J. (1980) Biophys. J. 29, 237—245
26 Simon, S., Stone, W.L. and Busto-Latorre, P. (1977) Biochim. Biophys. Acta 468, 378—388
27 Hunt, G.R. and Tipping, L.R.H. (1978) Biochim. Biophys. Acta 507, 242—261
28 Lecuyer, H. and Dervichian (1969) J. Mol. Biol. 45, 39—57
29 LeNeveu, D.M., Rand, R.P., Parsegian, V.A. and Gingell, D. (1977) Biophys. J. 18, 209—230
30 Buldt, G., Gally, H.-U., Seelig, A., Seelig, J. and Zaccai, G. (1978) Nature 271, 182—184
31 Hui, F.K. and Barton, P.G. (1973) Biochim. Biophys. Acta 296, 510—517
32 Jähnig, F., Harlos, K., Vogel, H. and Eibl, H. (1979) Biochemistry 18, 1459—1467
33 Nagle, J.F. (1976) J. Membrane Biol. 27, 233—250
34 Yue, B.Y., Jackson, C.M., Taylor, J.A.G., Mingus, J. and Pethica, B.A. (1976) J. Chem. Soc. Faraday Trans. I 72, 2685—2693
35 Prince, A. (1966) Alloy Phase Equilibria, p. 100, Elsevier, Amsterdam
36 Lee, A.G. (1977) Biochim. Biophys. Acta 472, 285—344
37 Jain, M.K. and Wu, N.M. (1977) J. Membrane Biol. 34, 157—207
38 Klevens, H.B. (1950) Chem. Rev. 1—78